Magnetic order in the double pyrochlore $Tb_2Ru_2O_7$

2010 J. Phys.: Condens. Matter 22 076003

(http://iopscience.iop.org/0953-8984/22/7/076003)

J. Phys.: Condens. Matter **22** (2010) 076003 (5pp) doi:10.1088/0953-8984/22/7/076003

Magnetic order in the double pyrochlore $Tb_2Ru_2O_7$

L J Chang[1], M Prager[2], J Perßon[2], J Walter[3], E Jansen[3], Y Y Chen[4] and J S Gardner[5]

[1] Nuclear Science and Technology Development Center, National Tsing Hua University, Hsinchu 30013, Taiwan
[2] Institut fuer Festkoerperforschung, Forschungszentrum Jülich, 52425 Jülich, Germany
[3] Mineralogisch-Petrologisches Institut, Universität Bonn, Außenstelle im Forschungszentrum Jülich, MIN/ZFR, 52425 Jülich, Germany
[4] Institute of Physics, Academia Sinica, Nankang Taipei 115, Taiwan
[5] Department of Physics, Indiana University, 2401 Milo B. Sampson Lane, Bloomington, IN 47408, USA

E-mail: ljchang@mx.nthu.edu.tw

Received 29 October 2009, in final form 2 January 2010
Published 29 January 2010
Online at stacks.iop.org/JPhysCM/22/076003

Abstract

Polycrystalline $Tb_2Ru_2O_7$ has been studied using dc susceptibility, specific heat and neutron scattering techniques. The high temperature paramagnetic state is dominated by the single ion character of Tb^{3+} and very similar to that of the well-studied spin liquid $Tb_2Ti_2O_7$. However, both the Ru^{4+} and Tb^{3+} sublattices order, at about 110 K and 3.5 K, respectively. Although the Tb sublattice does not fully order until 3.5 K, it is polarized in the presence of the internal field generated by the Ru^{4+} sublattice and possesses a significant moment at 7 K. Magnetic entropy measurements suggest that four levels exist in the first 30 K and inelastic neutron scattering investigations revealed two more levels at 10 and 14 meV. As the magnetic sublattices order, the excitations are perturbed from that measured in the paramagnetic state. These data are compared to data for other terbium based and double pyrochlores.

(Some figures in this article are in colour only in the electronic version)

Pyrochlore oxides of the chemical formula $A_2B_2O_7$, where A is a trivalent rare-earth ion and B is a tetravalent transition-metal ion, have the face-centered-cubic structure with space group $Fd\bar{3}m$ [1]. Due to the spatial arrangement of the metallic ions, two independent networks of corner-sharing tetrahedra, these compounds have attracted a lot of attention recently. If either A or B is magnetic this can lead to geometrical frustration and interesting low temperature magnetic properties, which are of great interest to both experimental and theoretical physicists. For example, $Ho_2Ti_2O_7$ had been identified as a spin ice [2, 3], $Gd_2Sn_2O_7$ is a good realization of a Heisenberg spin on this frustrating lattice [4], $Y_2Mo_2O_7$ is a spin glass with almost no disorder [5] and $Tb_2Ti_2O_7$ is a fluctuating spin liquid state at low temperature [6–9].

In the rare-earth ruthenates, the partially filled 4d shell of Ru^{4+} means both sublattices possess a magnetic moment producing two individual networks of magnetic corner-sharing tetrahedra. It has been reported that all the $RE_2Ru_2O_7$ (RE = rare-earth and Y) pyrochlores show a specific heat jump in the temperature range 75–160 K, where the transition temperature is correlated with the ionic size of the rare-earth [10–13]. This specific heat jump was explained as the freezing of the Ru moments into an antiferromagnetically coupled state which macroscopically exhibiting glass-like character due to the frustration [14]. Neutron diffraction on a few samples have confirmed this scenario [10, 15–19]. In $Ho_2Ru_2O_7$, susceptibility data [11] shows a slight irreversibility in zero-field cooled and field cooled data below 95 K, which is in very good agreement with the transition observed in specific heat measurements [10]. At a significantly lower temperature (3 K) specific heat shows a broad feature ubiquitous to many other frustrated rare-earth systems where strong, short range correlations exist and then a sharp, lambda-like transition can be seen as the Ho^{3+} sublattice orders [16]. This Ho^{3+} ordering was later observed by neutron scattering techniques and it was suggested that the

frustration is overcome by the internal field produced by the Ru^{4+} ordering [17] resulting in an ordered spin ice structure. This and other double pyrochlore studies [10–19] suggest the extended interactions associated with the 4d electrons of the B-site metal not only results in a higher ordering temperature but it also influences the A-site ion. These studies motivated us to investigate other double pyrochlores, where A and B are magnetic, to elucidate the ordering mechanism of the two frustrated sublattices. Here we report dc susceptibility, specific heat and neutron scattering results on $Tb_2Ru_2O_7$. Ru^{4+} orders at about 110 K and Tb^{3+} follows at 3.5 K. To our knowledge this is the first reporting of long range order of Tb^{3+} in $Tb_2Ru_2O_7$. Taira *et al* [13] reported a similar cusp in the susceptibility but concluded this was a result of short range correlations. Our neutron diffraction rules this out and when the data is compared to that of the spin liquid $Tb_2Ti_2O_7$, it shows the importance of the A–B coupling.

Polycrystalline $Tb_2Ru_2O_7$ samples were synthesized by the conventional solid-state reaction methods. High purity starting materials Tb_4O_7 and RuO_2 were mixed in stoichiometric proportions, heated at 850 °C for 24 h, pressed into pellets, and then sintered at 1150 °C for 48 h. Because of the high volatility of RuO_2, the sintering process was performed with the samples sealed in a quartz tube. The neutron and x-ray powder diffraction revealed no impurity in the samples within sensitivity limits of a few per cent, showed the samples had cubic symmetry at all temperatures studies, a lattice constant of 10.200(1) Å at room temperature and an oxygen content of 6.9 ± 0.1.

The magnetic properties were measured using a commercially available SQUID magnetometer in the temperature range of 1.7–300 K. The dc susceptibility, χ, measured in the applied field of 2 mT and the inverse susceptibility $\chi^{-1}(T)$ are shown in figure 1. The high temperature data ($T >$ 200 K) is described well by the Curie–Weiss (CW) law with an effective paramagnetic moment of 9.8 μ_B mol^{-1}, and the effective CW temperature −16.1 K, which are comparable to the values from $Tb_2Ti_2O_7$ [6]. We are not able to separate decisively the moment contributions from Tb^{3+} and Ru^{4+} in this measurement, but assuming this pyrochlore ruthenate like others, has approximately 1 μ_B on the ruthenium ion [15, 17], then approximately 9 μ_B would be on the terbium ion. This is consistent with the neutron refinements discussed later. The magnetic ordering of Ru^{4+}, which occurs at about 110 K, does not show a dramatic anomaly in the magnetization, presumably because the bulk properties are dominated by the larger Tb^{3+} moment. The data, however, does deviate from the CW fit at approximately 110 K, coinciding with the magnetic ordering of the Ru^{4+} [10]. As the temperature is lower a cusp can be seen around 3.5 K in the magnetization. This low temperature transition has not been reported earlier in the literature and was immediately assumed to be a result of the ordering of the Tb^{3+} lattice. One should remember that an identical Tb^{3+} sublattice exists in $Tb_2Ti_2O_7$ [6], where the large Tb^{3+} moment remains dynamic down to 17 mK. It can therefore be assume that the frustration is relieved due to the internal field associated with the Ru^{4+} sublattice, a similar conclusion was reached in $Ho_2Ru_2O_7$ [16, 17]. By applying a higher field,

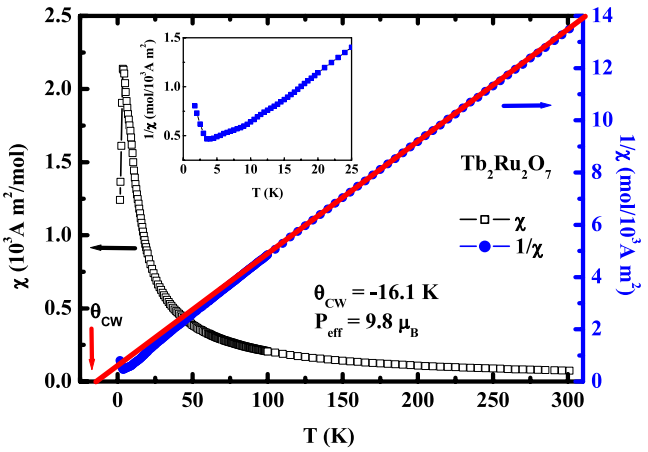

Figure 1. DC susceptibility χ measured at the applied field of 2 mT and the inverse susceptibility χ^{-1} for $Tb_2Ru_2O_7$. Curie–Weiss (CW) law fitted at high temperature (above 200 K) on the susceptibility data indicated that the effective paramagnetic moment 9.8 μ_B mol^{-1} and the effective CW temperature −16.1 K. The inset shows the inverse susceptibility χ^{-1} at low temperatures. The anomaly deviating from the linear χ^{-1} was observed below 15 K.

this transition is driven to a lower temperature, confirming its antiferromagnetic character (not shown in the figure). At 2 K, a saturated magnetic moment was determined from applied field versus magnetization measurements to be 5.4 μ_B (not shown). This value is very close to the results obtained from neutron diffraction, to be discussed later. The inset of figure 1 shows the inverse susceptibility χ^{-1} of low temperatures where the data can be seen to deviate from linearity below 15 K. This temperature can be correlated with a sharp increase in the intensity of magnetic Bragg peaks, see figures 2(a) and (b), far away from the phase transition of the Tb sublattice takes place and consistent with the broad feature seen in specific heat and discussed later in this paper.

Neutron powder diffraction experiments were carried out at SV-7, FRJ-II reactor, Jülich using 1.096 Å neutrons and a helium bath cryostat to control the sample temperatures between 1.5 and 270 K. Figure 2(a) displayed the neutron diffraction spectra of different temperatures and the Miller indices of the observed peaks at the lowest temperature. It should be noted here that, although indexed to a cubic unit cell, the magnetic Bragg scattering is not consistent with the $Fd\bar{3}m$ space group. It was noted that the strength of the magnetic scattering, which is proportional to the square of the magnetic moment, increased continuously with decreasing temperature below 110 K. This is illustrated in figure 2(b), where the intensities of the (1 1 1) Bragg peak is plotted as a function of temperature. Above 110 K, in the paramagnetic state the intensity is zero (or very small), due to the structure factor of the nuclear cell. Below 80 K, the data cannot be accounted for by the Ru sublattice alone and below 70 K we have determined that the majority of the magnetic scattering originates from the Tb^{3+} sublattice which is polarized by the Ru^{4+} ordering as being observed in other pyrochlore compounds by other groups [18–20]. Other magnetic peaks, including the (1 1 0) and (1 0 0) only emerge out of the background below 3.5 K

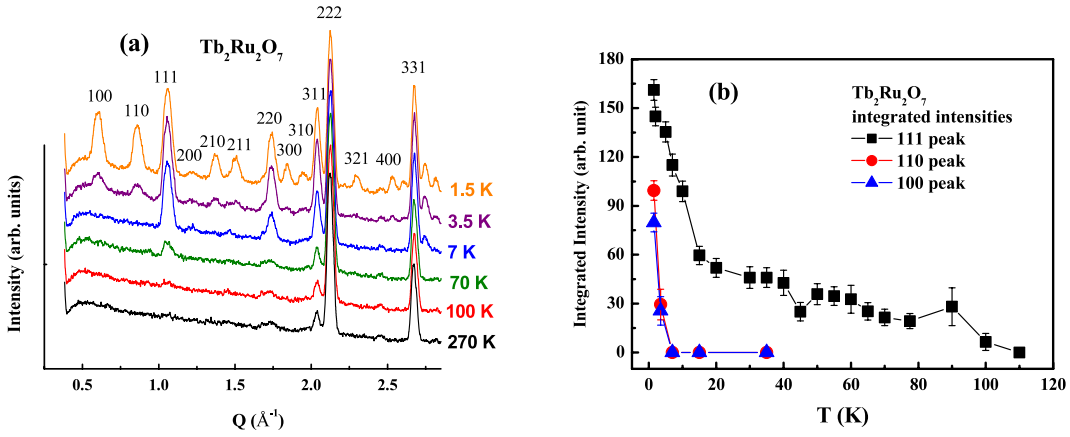

Figure 2. (a) The neutron diffraction spectra of different temperatures plotted with 70% y-scale offset for clarity. The low temperature diffraction pattern has also been indexed. (b) The integrated intensities of the magnetic peak (1 1 1), (1 1 0) and (1 0 0) from 1.5 to 110 K. Note the (1 1 1) grows continuously, long after the Ru^{4+} moment has saturated and the other reflections do not grow until true long range order is achieved on the Tb sublattice.

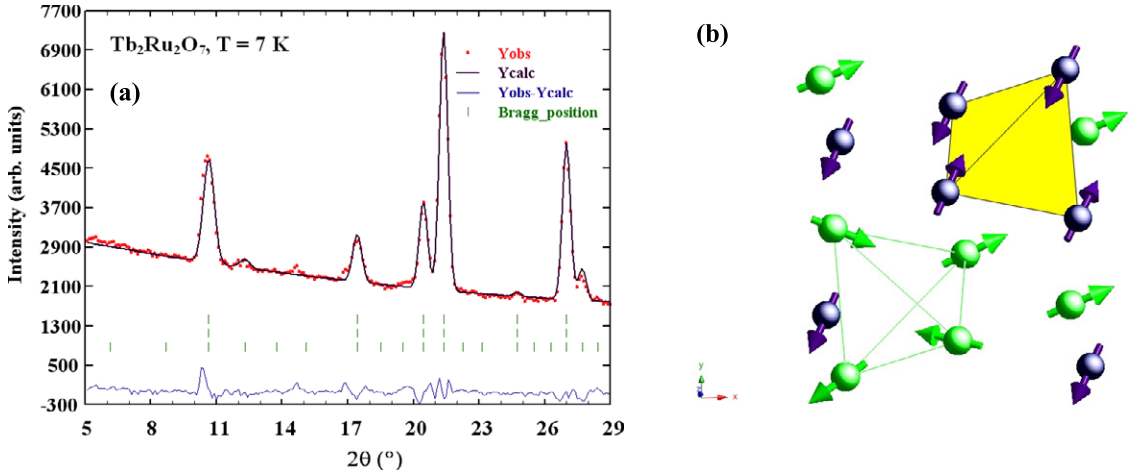

Figure 3. (a) The best fit to the low Q, data at 7 K. The upper tic marks represent the position of the nuclear Bragg peaks for the $Fd\bar{3}m$ cubic space group, while the middle and lower tic marks represent the magnetic scattering from Ru and Tb respectively. (b) The possible model used in the Rietveld refinement shown in (a) at 7 K. The gray spheres and solid tetrahedron represents the Tb moments and the Ru is represented by the green (light gray) spheres and open tetrahedron. Oxygen atoms are left out for clarity.

and they are a result of static, long ranged correlations in the Tb^{3+} sublattice, see figure 2(b).

Rietveld refinements were carried out on the 7 and 1.5 K data using the program, *Fullprof* [21]. A good fit was achieved to the 7 K data as shown in figure 3(a). The model that best describes the 7 K data is shown in figure 3(b). The Ru^{4+} moment can be described by 3 orthogonal vectors ($m_x = 0.76\ \mu_B$, $m_y = 0.25\ \mu_B$, $m_z = 0.19\ \mu_B$) resulting in a total moment of 0.9(1) μ_B. This, however, does not account for the entire magnetic scattering and a moment of 3.1(1) μ_B is required on the Tb^{3+} ion ($m_x = 1.12\ \mu_B$, $m_y = 2.80\ \mu_B$, $m_z = 0.81\ \mu_B$) to describe the data well. The total moment of Ru^{4+} is close to that published for other ruthenium pyrochlores, including $Y_2Ru_2O_7$ and $Nd_2Ru_2O_7$ [15] and $Ho_2Ru_2O_7$ [17] also obtained from neutron diffraction. The small Ru^{4+} moment may indicate that the Ru^{4+} is in the almost long range ordered state [15], or that not all of the Ru^{4+} moments are ordered [17]. The data at 1.5 K, however, was much harder to describe and no satisfactory model was found. At first glance it appears similar to $Tb_2Ti_2O_7$ under high pressure and low temperature [22], however, this model resulted in a poor fit. Any refinement, allowing all spins to vary, resulted in unrealistic moment sizes, so we fixed the Ru sublattice to that found at 7 K. The terbium ion was than found to be $\sim$5.2 μ_B in our best fits, but several key peaks, including the (2 0 0) and (3 1 1) Bragg peaks, were not described well. This model required an enlarged Tb basis (four tetrahedral) and two types of Tb moments, similar to that seen for Gd^{3+} in $Gd_2Ti_2O_7$ [23–25]. A 5.2 μ_B moment is however consistent with our applied field versus magnetization measurements and calculation by Gingras *et al* for $Tb_2Ti_2O_7$ [6]. The poor fit might result from the unrealistic constraint we imposed on the Ru moments or an incorrect structure for the Tb sublattice. More work is needed here, either single crystal studies or polarized neutron experiments, to determine the exact nature of the ordered state below 3 K.

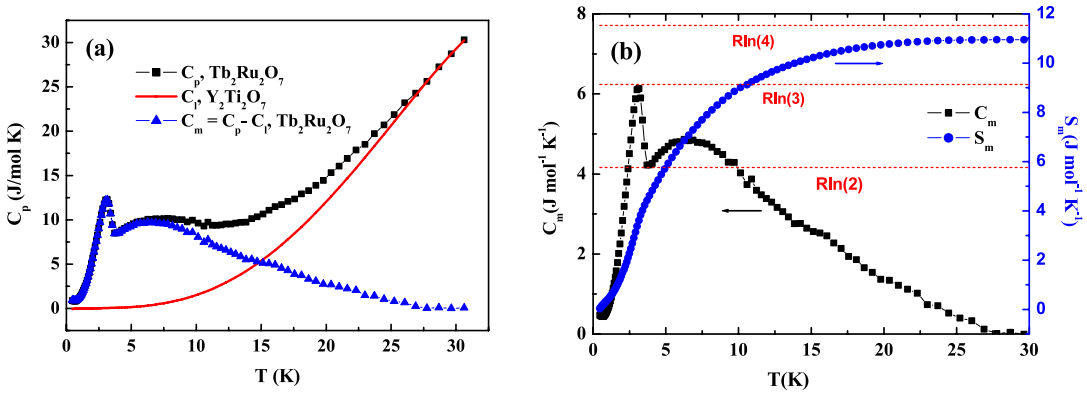

Figure 4. (a) Specific heat of $Tb_2Ru_2O_7$ between 0.5 and 30 K. The magnetic specific heat C_m of $Tb_2Ru_2O_7$ was calculated by subtracting the lattice contribution which was estimated by scaling the specific heat curve of $Y_2Ti_2O_7$ at 30 K. (b) The integrated magnetic entropy S_m of $Tb_2Ru_2O_7$. The accumulated entropy approaches to the value of $R \ln 4$ at 30 K.

Low temperature heat capacity was measured by using a standard thermal relaxation method between 0.5 and 30 K. The lattice contribution was estimated by scaling the specific heat curve of $Y_2Ti_2O_7$, as shown in figure 4(a), resulting in the magnetic specific heat C_m of $Tb_2Ru_2O_7$. A low temperature hyperfine contribution, normally observed in Tb-based compounds was not observed in our measurements, probably because of the 0.5 K base temperature [26, 27]. Similar to the magnetic specific heat C_m of $Tb_2Ti_2O_7$, the broad peak approximately centered at 6 K results from the short range correlations that exist between neighboring Tb moments at these temperatures [6]. A sharp peak at 3 K (figure 4(a)) is clear evidence of a phase transition and is concomitant with the appearance of magnetic Bragg peaks associated with Tb ordering. Integrating up the magnetic contribution results in the entropy, S_m of $Tb_2Ru_2O_7$, as shown in figure 4(b). The accumulated entropy approaches to the value of $R \ln 4$ at 30 K elucidating the presence of four low lying levels in the excitation spectrum. To get more information about these low lying excitations we performed inelastic neutron scattering (INS) experiments.

The time-of-flight spectrometer SV-29 at FRJ-II, Jülich, was used for the INS experiments. These experiments can provide data on excitations such as, phonons, magnons and crystal field. A closed-cycle cryostat was employed to control the temperature range between 2.4 and 120 K during the experiments. The results are shown in figure 5 for an incident neutron wavelength of 1.59 Å or 32.4 meV. In this polycrystalline experiment observing dispersive modes would be difficult, and we saw no evidence of dispersion. However, two non-dispersive crystalline electric field modes were observed at 10 and 14 meV. To improve statistics the data shown in figure 5 are summed over all Qs measured. These two peaks soften as the temperatures increase and spin–spin correlations decrease. Since the local Tb^{3+} environment is very similar to that in $Tb_2Ti_2O_7$ these modes are likely to be two singlet crystal field levels measured and identified in $Tb_2Ti_2O_7$ [6, 28]. With this energy resolution there is some indication of line broadening and thus a low lying excitations around 2 meV, that harden as the temperature is lowered through the terbium ordering temperature. Further

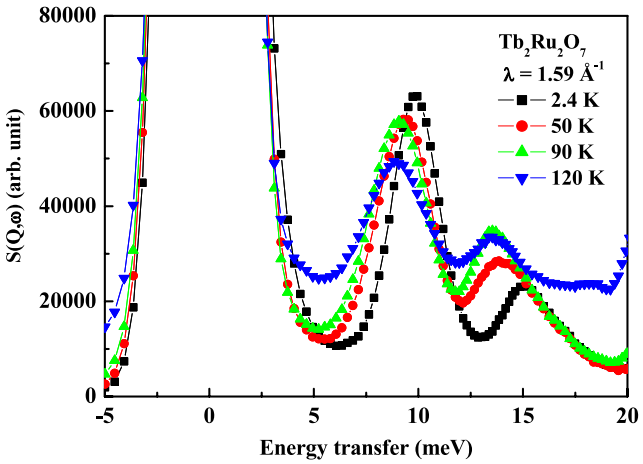

Figure 5. Inelastic neutron scattering results form $Tb_2Ru_2O_7$ 2.4, 50, 90, and 120 K. At 2.4 K, there is clearly some spectral weight at ∼2 meV, possibly from a low lying excitation not resolved in this experiment. Other, high energy excitations, are seen to shift as the temperature varies and spin–spin correlations within the sample change. Similar plots (not shown), summed over smaller Q ranges showed no dispersion at any given temperature.

measurements are required to confirm this and to determine the compete CEF Hamiltonian, but the magnetic entropy confirms four modes are expected below 3 meV.

In conclusion, we have carried out a variety of measurements on $Tb_2Ru_2O_7$ to understand the magnetic character of this frustrated magnet. Specific heat and neutron scattering have confirmed the ruthenium sublattice ordering at about 110 K, which is considerably lower than that expected by the −1200 K Curie–Weiss temperature, measured for Ru^{4+} in $Y_2Ru_2O_7$ [29]. This suppression of the ordering temperature from that predicted by mean field theory is typical of frustrated systems.

The bulk magnetic properties are dominated by the large Tb^{3+} ion, which has a single ion character similar to that in $Tb_2Ti_2O_7$. The influence of the Ru^{4+} sublattice is subtle in the high temperature paramagnetic regime, however it becomes more influential as the system is cooled. Below 80 K, evidence

of Tb–Ru correlations and a polarized Tb sublattice is seen in the magnetic neutron diffraction and a deviation from the Curie–Weiss law. These correlations grow as the temperature is lowered resulting in broad features in specific heat and neutron diffraction. Eventually the Tb lattice orders at 3.5 K, where new magnetic Bragg peaks are observed and concomitantly a peak is seen in specific heat and magnetic susceptibility. This is the first reported evidence of long range magnetic order of the Tb sublattice in the title compound. The approximate value of $R \ln 4$ in the accumulated magnetic entropy suggests the existence of four CEF energy levels within the first 30 K or ∼3 meV and two more are seen by neutron scattering at 10 and 14 meV. More studies are clearly needed to elucidate the true nature of the magnetic ground state of $Tb_2Ru_2O_7$ and the crystal field Hamiltonian associated with the Tb^{3+} ion. However, it is clear that this double pyrochlore provides scientists with new information that sheds light on the effects of geometrical frustration in pyrochlore oxide systems.

Acknowledgment

This work was supported by the National Science Council, Taiwan under the project number NSC 96-2739-M-213-001.

References

[1] Subramanian M A, Aravamudan G and Subba Rao G V 1983 *Prog. Solid State Chem.* **15** 55
[2] Harris M J, Bramwell S T, McMorrow D F, Zeiske T and Godfrey K W 1997 *Phys. Rev. Lett.* **79** 2554
[3] Bramwell S T and Gingras M J P 2001 *Science* **294** 1495
[4] Stewart J R, Gardner J S, Qiu Y and Ehlers G 2008 *Phys. Rev.* B **78** 132410
[5] Gardner J S, Gaulin B D, Lee S-H, Broholm C, Raju N P and Greedan J E 1999 *Phys. Rev. Lett.* **83** 211
[6] Gingras M J P, den Hertog B C, Faucher M, Gardner J S, Dunsinger S R, Chang L J, Gaulin B D, Raju N P and Greedan J E 2000 *Phys. Rev.* B **62** 6496
[7] Enjalran M and Gingras M J P 2004 *Phys. Rev.* B **70** 174426
[8] Gardner J S, Dunsiger S R, Gaulin B D, Gingras M J P, Greedan J E, Kiefl R F, Lumsden M D, MacFarlane W A, Raju N P, Sonier J E, Swainson I and Tun Z 1999 *Phys. Rev. Lett.* **82** 1012
[9] Molavian H R, Gingras M J P and Canals B 2007 *Phys. Rev. Lett.* **98** 157204
[10] Ito M, Yasui Y, Kanada M, Harashina H, Yoshi S, Murata K, Sato M, Okumura H and Kakurai K 2001 *J. Phys. Chem. Solids* **62** 337
[11] Bansal C, Kawanaka H, Bando H and Nishihara Y 2002 *Phys. Rev.* B **66** 52406
[12] Taira N, Wakeshima M and Hinatsu Y 2000 *J. Solid State Chem.* **152** 441
[13] Taira N, Wakeshima M and Hinatsu Y 2002 *J. Mater. Chem.* **12** 1475
[14] Lee J S, Noh T W, Bae J S, Yang I S, Takeda T and Kanno R 2004 *Phys. Rev.* B **69** 214428
[15] Ito M, Yasui Y, Kanada M, Harashina H, Yoshii S, Murata K, Sato M, Okumura H and Kakurai K 2000 *J. Phys. Soc. Japan* **69** 888
[16] Gardner J S, Cornelius A L, Chang L J, Prager M, Brückel Th and Ehlers G 2005 *J. Phys.: Condens. Matter* **17** 7089
[17] Wiebe C R, Gardner J S, Kim S-J, Luke G M, Wills A S, Gaulin B D, Greedan J E, Swainson I, Qiu Y and Jones C Y 2004 *Phys. Rev. Lett.* **93** 076403
[18] Taira N, Wakeshima M, Hinatsu Y, Tobo A and Ohoyama K 2003 *J. Solid State Chem.* **176** 165
[19] Gardner J S and Ehlers G 2009 *J. Phys.: Condens. Matter* **21** 436004
[20] Rule K C, Ruff J P C, Gaulin B D, Dunsiger S R, Gardner J S, Clancy J P, Lewis M J, Dabkowska H A, Mirebeau I, Manuel P, Qiu Y and Copley J R D 2006 *Phys. Rev. Lett.* **96** 177201
[21] *FullProf* suite web: http://www.ill.eu/sites/fullprof/
[22] Mirebeau I, Goncharenko I N, Cadavez-Peres P, Bramwell S T, Gingras M J P and Gardner J S 2002 *Nature* **420** 54
[23] Stewart J R, Ehlers G, Wills A S, Bramwell S T and Gardner J S 2005 *J. Phys.: Condens. Matter* **16** L321
[24] Champion J D M, Wills A S, Fennell T, Bramwell S T, Gardner J S and Green M A 2001 *Phys. Rev.* B **64** 140407(R)
[25] Hassan A K, Levy L P, Darie C and Strobel P 2003 *Phys. Rev.* B **64** 214432
[26] Blöte H W J, Wielinga R F and Huiskamp W J 1969 *Physica* **43** 549
[27] Catanese C A, Skjeltorp A T, Meissner H E and Wolf W P 1973 *Phys. Rev.* B **8** 4223
[28] Gardner J S, Gaulin B D, Berlinsky A J, Waldron P, Dunsiger S R, Raju N P and Greedan J E 2001 *Phys. Rev.* B **64** 224416
[29] Kmiec R, Swiatkowska Z, Gurgul J, Rams M, Zarzycki A and Tomala K 2006 *Phys. Rev.* B **74** 104425